DOI: 10.1021/ma102051q

Macromolecules
ARTICLE

ATRP of Methacrylates Utilizing $Cu^{II}X_2$/L and Copper Wire

Andrew J. D. Magenau, Yungwan Kwak, and Krzysztof Matyjaszewski*

Center for Macromolecular Engineering, Department of Chemistry, Carnegie Mellon University, 4400 Fifth Avenue, Pittsburgh, Pennsylvania 15213, United States

Received September 3, 2010; Revised Manuscript Received October 27, 2010

ABSTRACT: Methacrylate monomers were successfully polymerized by ATRP utilizing copper wire as an *in situ* reducing agent at near-ambient temperatures (35 °C). Well-controlled polymerizations were demonstrated with both PMDETA and dNbpy ligands. Polymerization rates, when conducted with PMDETA, were dependent on the surface area of Cu^0. Upon reduction of the copper deactivator concentration (i.e., $Cu^{II}Br_2$), polymerizations would only occur in the presence of excess ligand, whereas polymerization rates were independent of $[Cu^{II}Br_2]$. Proper selection of initiator and copper halide improved polymerization control with PMDETA. dNbpy was found to be an excellent ligand for MMA, resulting in polymerization systems with controlled behavior, predetermined molecular weights, narrow molecular weight distributions ($M_w/M_n \leq 1.2$), and near-quantitative initiation. The versatility of dNbpy was demonstrated by polymerization of a wide range of methacrylates, synthesis of polymethacrylates with molecular weights up to 80 000, and efficient chain extension of a PMMA macroinitiator.

Introduction

Atom transfer radical polymerization (ATRP) is one of the most versatile and robust controlled/living radical polymerization techniques, granting access to a diverse selection of precisely defined and complex polymeric architectures.[1−8] Control in ATRP is established by a dynamic equilibrium between a dormant species (R−X) and active propagating radical ($P^\bullet$) through a reversible redox process. Lower oxidation state catalysts (e.g., Cu^IX/L), typically based upon Cu,[1] Ru,[3] Fe,[9−11] Os,[12] and Mo[13,14] transition metals, act as activators by reducing alkyl halides and forming the corresponding oxidized transition metals (e.g., $Cu^{II}X_2$/L) and radicals. During this rapid reversible process, the halogen atom is homolytically transferred from the alkyl halide to transition metal, allowing the newly formed radical to temporarily propagate through vinyl monomers. The ATRP equilibrium ($K_{ATRP} = k_a/k_{da}$) essentially mediates the rate of polymerization (R_p), defined by eq 1, by ensuring steady and concurrent growth of all polymer chains, resulting in well-defined polymers with narrow molecular weight distributions. The rate constants of propagation, activation, and deactivation are identified as k_p, k_a, and k_{da}, respectively, in the following equation:

$$R_p = k_p[P^\bullet][M] = \frac{k_p k_a[R-X]_0[Cu^IX/L]}{k_{da}[Cu^{II}X_2/L]}[M] \qquad (1)$$

In the past decade, significant advancements to ATRP have been achieved. A variety of suitable polymerization conditions are now available, transcending traditional bulk, aqueous, and organic solutions to include heterogeneous systems of aqueous dispersed media,[15,16] emulsions,[17] miniemulsions,[18−20] microemulsions,[21] suspensions,[16] and dispersions.[22] Heterogeneous systems were in part possible due to activators generated by electron transfer (AGET) ATRP, a new catalytic activation process which introduced the concept of reducing air-stable deactivators (i.e., $Cu^{II}X_2$) to their corresponding activators (i.e., Cu^IX) *in situ* through addition of reducing agents (e.g., ascorbic acid, tin(II) 2-ethylhexanoate, hydrazine, Cu^0, etc.).[21] Furthermore, AGET led to improved protocols to provide significant catalyst reduction and simplified reaction setups. Recent developments have achieved diminished $Cu^{II}X_2$ catalyst concentrations between 1 and 10 ppm through activators regenerated by electron transfer (ARGET)[20,23−28] and initiators for continuous activator regeneration (ICAR) ATRP.[29−32] In these systems, Cu^IX activators are continuously regenerated from the $Cu^{II}X_2$ deactivators, a product of unavoidable termination events, in the presence of excess reducing agent (Scheme 1). Theoretically, the absolute concentration of copper catalyst can be decreased tremendously without affecting the polymerization rate as long as an adequate $[Cu^IX/L]/[Cu^{II}X_2/L]$ ratio is maintained (eq 1). Moreover, facile reaction setups for synthesis of advanced materials have been demonstrated in the presence of limited amounts of air, through eventual consumption of ambient oxygen species, without the need for specialized equipment further simplifying the ATRP process.[20]

Further to this point, zerovalent copper metal (e.g., copper powder or wire) serving as a reducing agent can offer many attractive advantages which include ppm concentrations of deactivator, reduced polymerization costs, improved tolerance to oxygen, facile reaction setup, and simple reducing agent removal. Utility of zerovalent copper to efficiently reduce $Cu^{II}X_2$ to Cu^IX in ATRP was first reported in 1997, whereby the authors demonstrated significant rate enhancements,[33] alkoxyamine synthesis,[34] polymerizations in the presence of oxygen[34] and at ambient temperatures with tris[2-(dimethylamino)ethyl]amine (Me_6TREN),[35] and its effectiveness in inimer (initiator−monomer)[36] and ionic liquid systems.[37] The vast majority of literature available today utilizing copper wire for controlled radical polymerization, entitled either ARGET ATRP[28,38] or single electron transfer living radical polymerization (SET-LRP),[39,40] have been preformed with acrylate monomers.

To date, a limited literature precedent exists for ATRP of methacrylate monomers, in the presence of Cu^0, therefore warranting development of such a protocol.[39,41−43] In one account,

*Corresponding author: Tel +1-412-268-3209; e-mail km3b@andrew.cmu.edu.

 Published on Web 11/15/2010

Scheme 1. ARGET and ICAR ATRP with Excess Reducing Agent

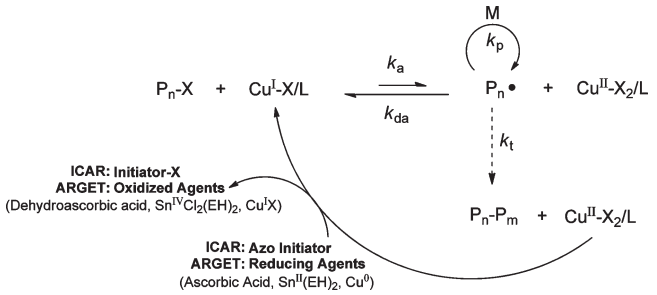

MMA was polymerized with sulfonyl halide initiators although polymerizations were plagued with low initiation efficiencies (ca. 54−69%), resulting in higher than expected molecular weight values.[41] Improvements were made by employing carbon tetrachloride as an initiator which increased initiation efficiency values between 67 and 91%, although peculiar kinetic behavior (i.e., acceleration) were observed in the semilogarithmic plots implying an increasing concentration of radical species.[41] Moreover, carbon tetrachloride can be considered as a difunctional initiating species;[44−46] an improper assumption of monofunctionality would lead to apparently higher initiation efficiencies. In a separate report, Perrier and co-workers demonstrated the necessity of $Cu^{II}Br_2$ deactivator to provide a well-controlled polymerization of MMA ($M_w/M_n \approx 1.30-1.35$) with zerovalent copper.[43] Polymerizations conducted without deactivator displayed a visible high molecular weight polymer fraction in gel permeation chromatography (GPC) and larger M_w/M_n values.

Herein, is reported a highly efficient and robust polymerization system for methacrylate monomers in nonpolar media. Simple reaction setup and easy catalyst removal can be accomplished with copper wire in addition to the convenience of near-ambient reaction temperatures (i.e., 35 °C). Copper complexes with *N,N,N′,N″,N″*-pentamethyldiethylenetriamine (PMDETA) and 4,4′-dinonyl-2,2′-bipyridine (dNbpy) ligands led to a well-controlled polymerization of MMA. Soluble copper complex concentrations between 250 and 500 ppm can be employed while still maintaining near-quantitative initiation, predetermined molecular weights, and polymerizations exhibiting controlled/living characteristics. The versatility of this approach was demonstrated by the following: (1) polymerization of a wide range of methacrylates, (2) achievement of molecular weights between 8000 and 80 000, and (3) chain extension of a PMMA macroinitatior. In this article emphasis is placed on synthetic aspects of ATRP to polymerize methacrylates with copper wire as a reducing agent. We report phenomenological effects of several reaction parameters on polymerization control and the resulting methacrylate polymers. More detailed mechanistic studies of this process will be reported elsewhere.

Experimental Section

Materials. Methyl methacrylate (MMA, 99%, Aldrich), ethyl methacrylate (EMA, 99%, Aldrich), butyl methacrylate (BMA, 99%, Aldrich), *tert*-butyl methacrylate (tBMA, 98%, TCI America), and methyl acrylate (MA, 99%, Aldrich) were passed through a column filled with basic alumina prior to use. Copper(II) bromide ($CuBr_2$, 99.999%, Aldrich), copper(II) chloride ($Cu^{II}Cl_2$, 99.999%, Aldrich), *N,N,N′,N″,N″*-pentamethyldiethylenetriamine (PMDETA, 99%, Aldrich), tris(2-pyridylmethyl)amine (TPMA, 98%, ATRP solutions), tris[2-(dimethylamino)ethyl]amine (Me_6TREN, 99%, ATRP solutions), 4,4′-dinonyl-2,2′-bipyridine (dNbpy, 97%, Aldrich), ethyl α-bromophenylacetate (EBPA, 97%, Aldrich), ethyl α-chlorophenylacetate (ECPA, 97%, Aldrich), ethyl bromoisobutyrate (EBiB, 98%, Aldrich), 2-bromopropionitrile (BPN, 97%, Aldrich), copper wire (d = 1 mm, Alfa Aesar), anisole (99%, Aldrich), DMF (≥99.9%, Aldrich), and DMSO (99.9%, Aldrich) were used as received.

Instrumentation. Molecular weight and M_w/M_n values were determined by gel permeation chromatography (GPC). The GPC was conducted with a Waters 515 HPLC pump and a Waters 2414 refractive index detector using PSS columns (Styrogel 10^2, 10^3, 10^5 Å) in tetrahydrofuran (THF) as an eluent at a flow rate of 1 mL/min at 35 °C. The column system was calibrated with 12 linear poly(methyl methacrylate) (M_n = 800−2 570 000) standards. ^{1}H NMR spectra were obtained in *d*-chloroform using a Bruker 300 MHz spectrometer with a delay time of 5 s.

General Procedure for Synthesis of Methacrylates by ATRP. A representative ATRP procedure is as follows. To a long-neck Schlenk style round-bottom flask equipped with a magnetic stir bar were charged 1.6 mL of anisole, 100 μL of 0.076 M $Cu^{II}Br_2$ and 0.149 M dNbpy in DMF, and 1.6 mL of 0.047 M EBPA in MMA. The resulting solution was then degassed with three freeze−pump−thaw cycles. After the last pump cycle, copper wire (L = 1 cm, d = 1 mm) was added under a nitrogen atmosphere, at which time the reaction was evacuated and backfilled with nitrogen three times. Next, the contents were allowed to thaw, and the final reaction mixture was submerged in an oil bath maintained at 35 °C. Samples were withdrawn periodically for ^{1}H NMR and GPC analysis for conversion and molecular weight determination, respectively.

PMMA Macroinitiator Synthesis. Poly(methyl methacrylate) (PMMA-Br) macroinitiator was prepared by following a similar procedures to that described above and as reported in Table 2 entry 11. ATRP of MMA was conducted with a formulation as follows: MMA/EBPA/dNbpy/$CuBr_2$ = 200/1/0.2/0.1 in 50% (v/v) anisole at 35 °C with 3.5 mm^2/ml copper wire and reaction volume of 10.3 mL. The polymerization was stopped after ∼5.8 h by opening the reaction vessel and exposing the contents to air. Afterward, the reaction mixture was immediately passed through a column filled with neutral alumina to remove the copper catalyst. Next, the polymer was precipitated twice against methanol and collected to obtain a white powder. The precipitated polymer was dried at room temperature under reduced pressure until a constant weight was obtained. PMMA-Br macroinitiator was then analyzed by GPC and ^{1}H NMR (M_n = 8000, M_w/M_n = 1.15 at 36% conversion).

Block Copolymer Synthesis by Chain Extension of PMMA-Br Macroinitiator. PMMA-*b*-PMA was synthesized as follows and with conditions summarized in Table 2 entry 12. To a long-neck Schlenk style round-bottom flask equipped with a magnetic stir bar were charged 0.178 g of PMMA-Br, 2 mL of MA, 2 mL of DMSO, and 100 μL of 0.022 M $Cu^{II}Br_2$ and 0.022 M PMDETA solution in DMSO. The resulting solution was then degassed with three freeze−pump−thaw cycles. After the last pump cycle, copper wire (L = 5 cm, d = 1 mm) was added under a nitrogen atmosphere, at which time the reaction was evacuated and backfilled with nitrogen three times. Next the contents were allowed to thaw, and the final reaction mixture was submerged in an oil bath maintained at 30 °C for ∼8 h. Samples were withdrawn periodically for ^{1}H NMR and GPC analysis for conversion and molecular weight determination, respectively. PMMA-*b*-PMA block copolymer was then analyzed by GPC (M_n = 71 900, M_w/M_n = 1.12 at 70% conversion).

Results and Discussion

ATRP of MMA was conducted utilizing copper wire as an *in situ* reducing agent according to Scheme 1. Near room temperature reaction conditions were targeted, and commercially available reagents were selected for all polymerizations presented in this work. Initial experimentation was designed to elucidate an appropriate copper ligand complex for the successful polymerization of MMA. Ligands with moderate to high ATRP equilibrium constant (K_{ATRP}), such as PMDETA, TPMA, and Me_6TREN,

Table 1. ATRP of MMA with PMDETA Utilizing Copper Wire[a]

expt no.	ATRP system	[M]/[I]/[L]/[$Cu^{II}Br_2$]	[Cu^{II}][b] (ppm)	[Cu^0]$_s$ (mm^2/mL)	time (h)	p[c] (%)	$M_{n,theo}$	$M_{n,GPC}$	M_w/M_n	I_{eff} (%)
1	MMA/EBPA/Me_6TREN/$Cu^{II}Br_2$	200/1/0.3/0.1	500	1.1	25.0	51	10 400	13 400	1.19	78
2	MMA/EBPA/TPMA/$Cu^{II}Br_2$	200/1/0.3/0.1	500	1.1	25.0	78	15 900	20 900	1.21	76
3	MMA/EBPA/PMDETA/$Cu^{II}Br_2$	200/1/0.5/0.5	2500	1.1	16.4	78	15 800	16 700	1.13	96
4	MMA/EBPA/PMDETA/$Cu^{II}Br_2$	200/1/0.5/0.5	2500	3.5	18.0	75	15 300	20 000	1.21	78
5	MMA/EBPA/PMDETA/$Cu^{II}Br_2$	200/1/0.5/0.5	2500	9.6	6.7	67	13 700	21 300	1.39	65
6	MMA/EBPA/PMDETA/$Cu^{II}Br_2$	200/1/0.5/0.5	2500	19	2.8	40	8 300	12 000	1.32	69
7	MMA/EBPA/PMDETA/$Cu^{II}Br_2$	200/1/0.1/0.1	500	1.1	19.0					
8	MMA/EBPA/PMDETA/$Cu^{II}Br_2$	200/1/0.2/0.1	500	1.1	24.4	68	13 800	16 300	1.12	85
9	MMA/EBPA/PMDETA/$Cu^{II}Br_2$	200/1/0.25/0.1	500	1.1	18.9	80	16 200	19 200	1.17	84
10	MMA/EBPA/PMDETA/$Cu^{II}Br_2$	200/1/0.3/0.1	500	1.1	24.4	93	18 800	24 400	1.15	77
11	MMA/EBPA/PMDETA/$Cu^{II}Br_2$	200/1/0.3/0.05	250	1.1	22.1	95	19 000	24 300	1.20	78
12	MMA/EBPA/PMDETA/$Cu^{II}Br_2$	200/1/0.3/0.025	125	1.1	22.3	93	18 600	23 300	1.20	80
13	MMA/EBPA/PMDETA/$Cu^{II}Br_2$	200/1/0.3/0.01	50	1.1	22.5	91	18 200	17 400	1.29	105
14	MMA/EBPA/PMDETA/$Cu^{II}Br_2$	200/1/0.3/0	0	1.1	27.5	98	19 900	24 900	1.28	79
15	MMA/BPN/PMDETA/$Cu^{II}Br_2$	200/1/0.3/0.1	500	1.1	13.1	88	17 900	20 800	1.20	86
16	MMA/EBiB/PMDETA/$Cu^{II}Br_2$	200/1/0.3/0.1	500	1.1	12.8	88	17 800	20 000	1.26	89
17	MMA/ECPA/PMDETA/$Cu^{II}Cl_2$	200/1/0.3/0.1	500	1.1	15.9	91	18 300	18 800	1.16	97

[a] All polymerizations were conducted with [M] = 4.55 M, T = 35 °C, 50% (v/v) anisole, total reaction volume of 3.3 mL, and copper wire (L = 2, 10, 30, and 60 mm, d = 1 mm). [b] Calculated by the initial molar ratio of $Cu^{II}X_2$ to monomer. [c] Determined by ^{1}H NMR.

Table 2. ATRP of MMA with dNbpy Utilizing Copper Wire[a]

expt no.	ATRP system	[M]/[I]/[L]/[$Cu^{II}Br_2$]	[Cu^{II}][b] (ppm)	[Cu^0]$_s$ (mm^2/mL)	time (h)	p[c] (%)	$M_{n,theo}$	$M_{n,GPC}$	M_w/M_n	I_{eff} (%)
1	MMA/EBPA/dNbpy/$Cu^{II}Br_2$	200/1/1.0/0.5	2500	3.5	10.1	77	15 700	16 700	1.16	94
2	MMA/EBPA/dNbpy/$Cu^{II}Br_2$	200/1/0.2/0.1	500	3.5	28.0	93	19 000	19 900	1.13	95
3	MMA/EBPA/dNbpy/$Cu^{II}Br_2$	200/1/0.1/0.05	250	3.5	28.0	75	15 300	15 000	1.14	102
4	MMA/EBPA/dNbpy/$Cu^{II}Br_2$	200/1/0.02/0.01	50	3.5	28.0	72	14 600	12 300	1.21	120
5	MMA/EBPA/dNbpy/$Cu^{II}Br_2$	200/1/0.2/0	0	3.5	27.5	94	19 000	19 300	1.14	98
6	MMA/EBPA/dNbpy/$Cu^{II}Br_2$	600/1/0.2/0.1	170	3.5	32.0	88	53 000	50 600	1.16	105
7	MMA/EBPA/dNbpy/$Cu^{II}Br_2$	1000/1/0.2/0.1	100	3.5	32.0	83	83 200	78 500	1.23	106
8	EMA/EBPA/dNbpy/$Cu^{II}Br_2$	200/1/0.2/0.1	500	3.5	45.8	94	21 800	20 800	1.11	105
9	BMA/EBPA/dNbpy/$Cu^{II}Br_2$	200/1/0.2/0.1	500	3.5	31.2	97	27 800	25 300	1.09	109
10	tBMA/EBPA/dNbpy/$Cu^{II}Br_2$	200/1/0.2/0.1	500	3.5	30.8	79	22 600	22 500	1.14	100
11	MMA/EBPA/dNbpy/$Cu^{II}Br_2$	200/1/0.2/0.1	500	3.5	5.8	36	7 400	8 000	1.15	92
12	MA/MI-10/PMDETA/$Cu^{II}Br_2$	1000/1.0/0.1/0.1	100	13	8.0	70	68 300	71 900	1.12	94[d]

[a] All polymerizations, except entries 11 and 12, were conducted with [M] 4.55 M, T = 35 °C, 50% (v/v) anisole, total reaction volume of 3.3 mL, and copper wire (L = 10 and 50 mm, d = 1 mm). [b] Calculated by the initial molar ratio of $Cu^{II}X_2$ to monomer. [c] Determined by ^{1}H NMR. [d] Blocking efficiency = $(M_{n,theo/block\ copolymer} - M_{n,GPCmacroinitiator})/(M_{n,GPC/block\ copolymer} - M_{n,GPCmacroinitiator}) \times 100$.

were briefly investigated. Copper complexes with these ligands were able to catalyze ATRP of MMA, and the polymerization results are summarized in Table 1 (entries 1, 2, and 10). Conversion values reported in Tables 1 and 2 are designated as the symbol "p". In the case of Me_6TREN and TPMA, limited conversions and slightly higher M_w/M_n values in comparison to PMDETA resulted. The relative levels of control with each ligand may, in part, be rationalized by the [Cu^IBr] and [$Cu^{II}Br_2$] complexes and overall activity of the Cu^IBr/L complex for each ligand system. Concentrations of reduced catalyst would be expected to be lowest for Me_6TREN, slightly higher for TPMA, and the highest for PMDETA, originating from their redox potentials and relative K_{ATRP} values. In contrast, Cu^IBr complexes with Me_6TREN and TPMA are most active and should lead to very fast activation, especially with large K_{ATRP} monomers and initiators (i.e., methacrylates). On the basis of the conversion and M_w/M_n values, PMDETA, the least active among these ligands, appeared to be most appropriate for further investigation.

Investigation of the Effect of Copper Wire Length, [PMDETA], and [$Cu^{II}Br_2$]. Cu^0 in the presence of ligand can produce Cu^IBr through both direct activation of alkyl halides and comproportionation with $Cu^{II}Br_2$.[47] Therefore, a series of reactions shown in Table 1 (entries 3−6) were designed to gain insight into the effect of copper wire length. For all reactions, the "concentration" of copper wire (i.e., [Cu^0]$_s$) is described as surface area per volume (mm^2/mL) assuming the copper wire area is represented by a regular cylinder. Varying the [Cu^0]$_s$ from ca. 1.1 to 19 mm^2/mL revealed three general trends. First, increased [Cu^0]$_s$ resulted in lower obtainable conversions. Low [Cu^0]$_s$ (entries 3 and 4) reached conversion values greater than 75%, whereas high [Cu^0]$_s$ (entries 5 and 6) reached ultimate conversion values of ca. 40 and 67%, at which point, no further monomer conversion occurred with increased polymerization time (Figure 1a). Limited conversion is assumed to be a result of accumulated $Cu^{II}Br_2$ deactivator, a consequence of considerable termination events. Second, polymerizations with higher [Cu^0]$_s$ resulted in higher polymerization rates. This observation further bolsters our assumption of increased termination events because of an effectively larger concentration of propagating radicals. Last, broad molecular weight distributions, lower initiation efficiencies (I_{eff}), and decreased correlation between experimental and theoretical molecular weight values (Figure 1b) were observed as the [Cu^0]$_s$ was increased (Table 1, entries 3−6). This behavior can be correlated with a reduced [$Cu^{II}Br_2$] due to increased comproportionation with copper wire. Examination of Figure 1b reveals that further deviation from the targeted molecular weight occurs when using a larger [Cu^0]$_s$. Early termination events, evident from decreasing slopes in Figure 1a, results in a reduction in the concentration of living chain ends and concomitantly produces higher than expected molecular weight values, with exception of the 1.1 mm^2/mL system. Therefore, to obtain a controlled polymerization using

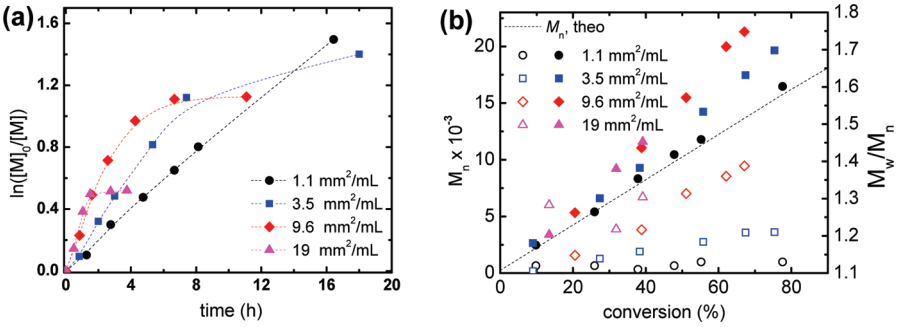

Figure 1. (a) First-order kinetic plot and (b) evolution of molecular weight (solid) and molecular weight distribution (hollow) versus conversion plot as a function of copper wire length. Polymerizations conducted in 50% (v/v) anisole at 35 °C. [MMA] = 4.55 M; [MMA]/[EBPA]/[PMDETA]/[$Cu^{II}Br_2$] = 200/1/0.5/0.5 (Table 1, entries 3−6).

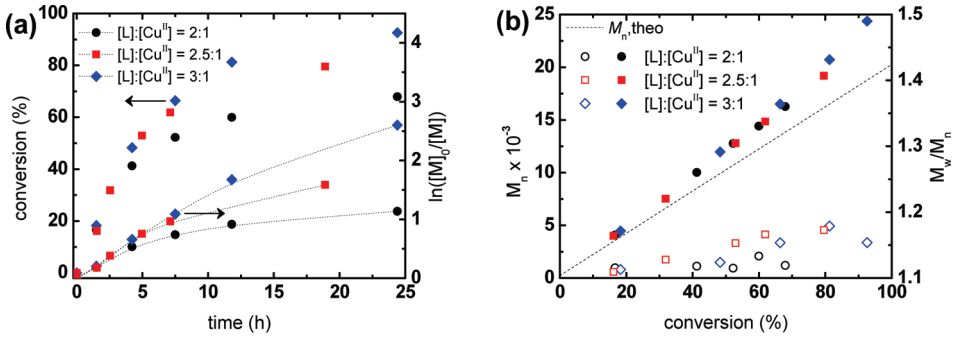

Figure 2. (a) Monomer conversion and first-order kinetic plots versus time (b) evolution of molecular weight (solid) and molecular weight distribution (hollow) versus conversion as a function of excess ligand over Cu^{II} deactivator concentration. Polymerizations conducted in 50% (v/v) anisole at 35 °C. [MMA] = 4.55 M; [MMA]/[EBPA]/[$Cu^{II}Br_2$] = 200/1/0.5; Cu^0: L = 2 mm, d = 1 mm (Table 1, entries 8−10).

PMDETA, a low $[Cu^0]_s$ must be used to reduce the concentration of propagating radicals and ultimately diminish the frequency of termination events. This concept was demonstrated by entry 3 where linear first-order kinetic behavior was observed (Figure 1a, solid and hollow circles), indicating a constant concentration of propagating species and a gradual increase in molecular weight with conversion matching closely to the theoretically predetermined values.

Upon reduction of the ligand and $Cu^{II}Br_2$ concentrations to 500 ppm (entry 7), no polymerization resulted after 19 h using conditions similar to entry 3. The overall reduction of deactivator, unavoidable termination events, and preferential binding of ligands to higher oxidation state copper[48,49] may each have been responsible for the absence of polymerization. In the situation where the vast majority of ligand is bound to $Cu^{II}Br_2$ and a limited amount is available to complex with $Cu^{I}Br$, additional ligand would be required to solubilize all copper species, specifically $Cu^{I}Br$ activators, to sustain a reasonable rate of polymerization. Ultimately, the total amount of soluble copper is controlled by the concentration of ligand. Indeed, when a 2-fold excess of ligand was introduced to the system ~70% of the monomer was consumed in 24 h (entry 8 and Figure 2a). A further increase in the [PMDETA] (entries 9 and 10) resulted in even larger conversion values. These results indicate that due to unavoidable termination events (i.e., formation of $Cu^{II}Br_2$) and generation of $Cu^{I}Br$ through comproportionation and activation of alkyl halides with copper wire, a proper excess of ligand must be used or the majority of soluble copper−ligand species will reside with $Cu^{II}Br_2$. In consequence, the [$Cu^{I}Br$/L]/[$Cu^{II}Br_2$/L] ratio will then become smaller and eventually retard the rate of polymerization (eq 1). Overall, with an excess of ligand (i.e., 3-fold to $Cu^{II}Br_2$) linear semilogarithmic kinetic behavior was observed until ca. 80% monomer conversion, and a narrow molecular weight distribution ($M_w/M_n < 1.2$) was maintained with moderate initiation efficiency (Figure 2a,b). It is noteworthy to mention that PMDETA, when used in excess to $Cu^{II}Br_2$, may also serve as a reducing agent.[50] A control reaction was conducted with PMDETA in conditions identical to those found in entry 10 of Table 1, except without copper wire. No polymerization was observed, after 24 h, confirming copper wire as the dominant reducing agent in these conditions.

Investigation of the Effect of Deactivator Concentration. Following the investigation of [PMDETA], the influence of [$Cu^{II}Br_2$] was examined between 500 and 50 ppm (entries 10−14). In all cases conversion values over 90%, initiation efficiencies ≥78%, and $M_w/M_n < 1.3$ were achieved. Likewise, polymerization rates were found to be similar in the early stages of polymerization until ca. 60% conversion (Figure 3a). This is consistent with ICAR/ARGET ATRP in the presence of excess reducing agent (e.g., AIBN, tin(II) 2-ethylhexanoate, ascorbic acid, etc.); polymerizations rates are not dictated by the concentration of copper catalyst but rather by the amount of reducing agent and relative concentration of [$Cu^{I}Br$/L] and [$Cu^{II}Br_2$/L].[20] Control began to deteriorate around a deactivator concentration of 50 ppm evident from the decreasing slope in the first-order kinetic plot, suggesting significant termination. In addition, loss of control was realized from a visible decrease in slope in the molecular weight versus conversion plot accompanied by a more pronounced increase in M_w/M_n values (Figure 3b; solid and hollow diamonds). Polymerization in the absence of deactivator (entry 14, solid and hollow stars) displayed conversion and polymerization rates similar to those of entries 10−13. This experiment maintained a similar correlation to the theoretical molecular

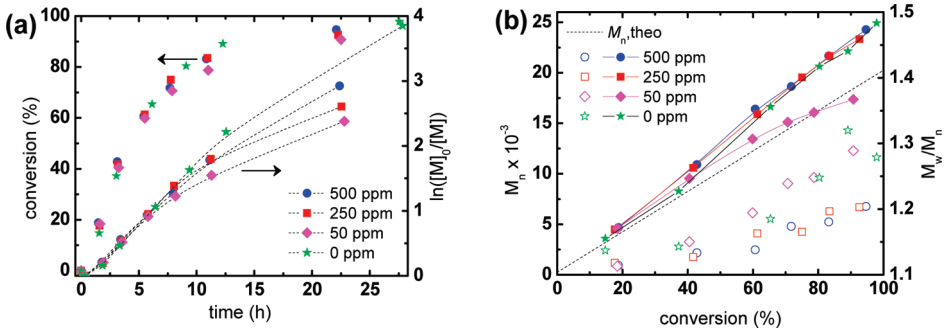

Figure 3. (a) Monomer conversion and first-order kinetic plots versus time; (b) evolution of molecular weight (solid) and molecular weight distribution (open) versus conversion as a function of [$Cu^{II}Br_2$]. Polymerizations conducted in 50% (v/v) anisole at 35 °C. [MMA] = 4.55 M; [MMA]/[EBPA]/[PMDETA] = 200/1/0.3; Cu^0: L = 2 mm, d = 1 mm (Table 1, entries 10−14).

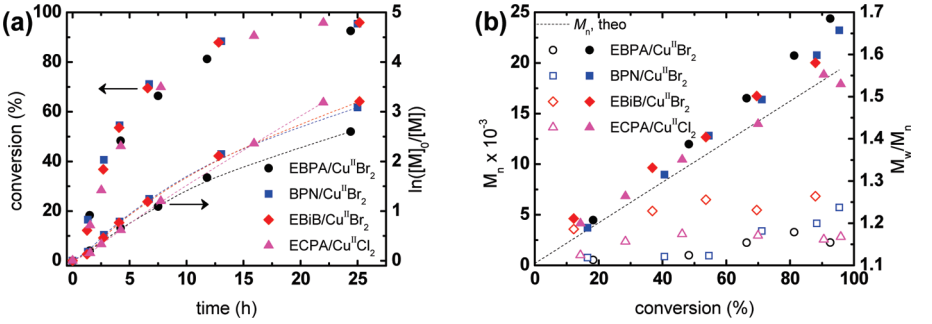

Figure 4. (a) Monomer conversion and first-order kinetic plots versus time; (b) evolution of molecular weight (solid) and molecular weight distribution (open) versus conversion as a function of initiator and/or copper halogen. Polymerizations conducted in 50% (v/v) anisole at 35 °C. [MMA] = 4.55 M; [MMA]/[PMDETA]/[$Cu^{II}X_2$] = 200/1/0.3/0.1; Cu^0: L = 2 mm, d = 1 mm (Table 1, entries 10, 15−17).

weight values as the 500 and 250 ppm systems, although larger M_w/M_n values of ~1.3 were observed analogous to the 50 ppm system.

Investigation of the Effect of Initiator Structure and Copper Halide. In an effort to improve initiation efficiencies and reduce termination events during polymerization, three different initiators were studied along with one chlorine analogue system of ethyl α-bromophenylacetate (EBPA)/$Cu^{II}Br_2$. With respect to the highly active EBPA, a moderate and lower activity initiator were selected: 2-bromopropionitrile (BPN) and ethyl 2-bromoisobutyrate (EBiB), respectively (entries 15 and 16).[28,51,52] The highly active EBPA may have flooded the polymerization with radicals in the early stages of polymerization and hence caused early termination and lower initiation efficiency values (entry 10, I_{eff} = 77%). Both BPN and EBiB had slightly higher final conversion values and polymerization rates but maintained similar linear first-order relationships with time to that of EBPA (Figure 4a). The most active EBPA produced more deactivator from termination, slowing the polymerization. BPN and EBPA lead to comparable M_w/M_n values during the majority of the polymerization with EBiB having the largest among all three. Agreements with theoretical molecular weights (I_{eff}) for BPN and EBiB were slightly improved as compared with EBPA (Figure 4b). A system containing either a very active (EBPA) or less active initiator (EBiB) resulted in early termination or slow initiation, respectively, as shown in Figure 5. BPN begins the polymerization with an I_{eff} value of ca. 95%, whereas for the more active initiator (EBPA), this value is around 87%. In both cases, though, radical termination continues to occur indicated by the slowly decreasing I_{eff} values. When observing EBiB, slow initiation is visible by the increase in I_{eff} values in the early stages of polymerization. Therefore, this intermediate initiator (i.e., BPN) provided

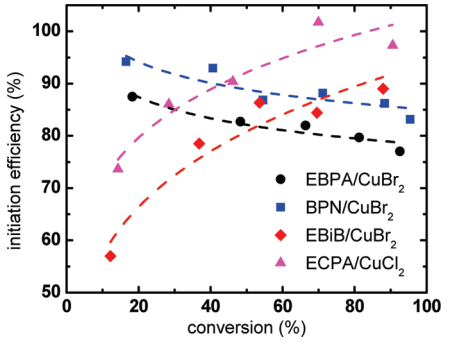

Figure 5. Initiation efficiency versus conversion for initiator and/or copper catalyst halide. Polymerizations conducted in 50% (v/v) anisole at 35 °C. [MMA] = 4.55 M; MMA/PMDETA/$Cu^{II}X_2$ = 200/1/0.3/0.1; Cu^0: L = 2 mm, d = 1 mm (Table 1, entries 9, 14−16).

the appropriate balance to maintain an initiation rate high enough over the propagation rate for spontaneous and uniform initiation while, at the same time, low enough to reduce early termination. Further improvement was accomplished by utilizing a slightly less active initiator, ECPA, and substitution of copper(II) bromide with a copper(II) chloride catalyst (entry 17). Kinetic data showed linear first-order behavior during the whole polymerization and demonstrated a significant improvement compared to its $Cu^{II}Br_2$/EBPA counterpart (Figure 4a). In addition, a narrow molecular weight distribution was maintained, theoretical and experimental molecular weight showed great correlation (Figure 4b), and initiation efficiency values were between 95 and 100% (entry 17 and Figure 5).

ATRP with dNbpy Ligand. Continued experimentation was focused toward using a lower K_{ATRP} ligand in hopes to

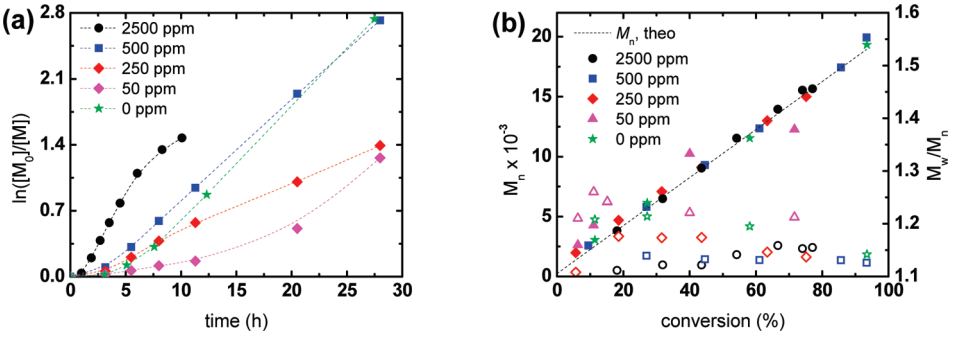

Figure 6. (a) First-order kinetic plot versus time; (b) evolution of molecular weight (solid) and molecular weight distribution (hollow) versus conversion as a function of [dNbpy] and [$Cu^{II}Br_2$]. Polymerizations conducted in 50% (v/v) anisole at 35 °C. [MMA] = 4.55 M; [MMA]/[EBPA] = 200/1; [dNbpy]/[$Cu^{II}Br_2$] = 2/1; Cu^0: L = 10 mm, d = 1 mm (Table 2, entries 1−6). Reaction conditions of entry 5 (stars) are identical to entry 2 (squares) except without $Cu^{II}Br_2$.

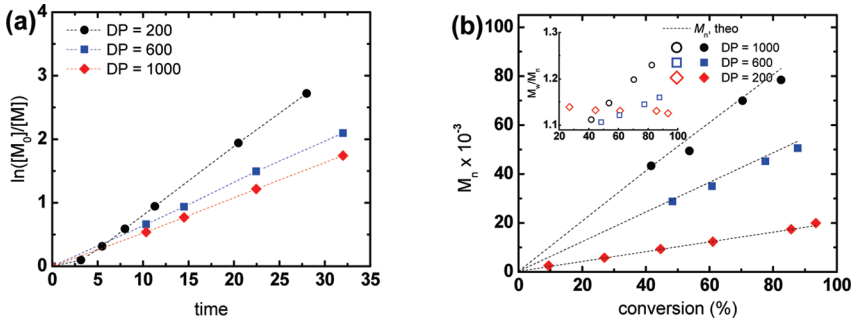

Figure 7. (a) First-order kinetic plot versus time; (b) molecular weight (solid) and molecular weight distribution (hollow) versus conversion as a function DP. Polymerizations conducted in 50% (v/v) anisole at 35 °C. [MMA] = 4.55 M; EBPA/dNbpy/$Cu^{II}Br_2$ = 1/0.2/0.1; Cu^0: L = 10 mm, d = 1 mm (Table 2, entries 2, 6, and 7).

further counteract the relative large ATRP equilibrium constant of MMA. Therefore, dNbpy was investigated and proved to be a versatile, robust, and effective ligand for the polymerization of MMA in the presence of copper wire. Initial experimentation focused on using relatively high concentrations of ligand and deactivator (i.e., 2500 ppm). The polymerization of MMA proceeded in a well-controlled fashion until ~65% conversion, when the polymerization rate began to decrease. Regardless, the outcome of this system gave excellent correlation between experimental and theoretical molecular weight vales, low M_w/M_n, and near-quantitative initiation (Table 2, entry 1, Figure 6a,b). Entries 2−4 were designed to reduce the concentration of ligand and deactivator to evaluate the required lower [$Cu^{II}Br_2$] limit to maintain control. Polymerization systems containing 500 and 250 ppm had diminished polymerization rates, while still maintaining linear first-order kinetic behavior, predetermined molecular weights, low M_w/M_n, and excellent initiation efficiencies ($I_{eff} \geq 94\%$). At 50 ppm of $Cu^{II}Br_2$ polymerization control was lost, indicated by the increasing slope in the first-order kinetic plot (Figure 6a) and decreasing slope in Figure 6b. Loss of control is mostly likely due to the low equilibrium constant of the dNbpy complex, which is unable to provide an adequate concentration of deactivator species at low concentrations (i.e., both dNbpy and $Cu^{II}Br_2$). An identical reaction to entry 2 was conducted without $Cu^{II}Br_2$ (entry 5, Figure 6, solid and hollow stars). Similar kinetic behavior was observed in the first-order semilogarithmic plot, although an induction period was observed in the early stages of polymerization from the slow generation of activator species. Strong correlations between experimental and theoretical molecular weights were evident; however, high M_w/M_n values existed until ca. 60% monomer conversion in comparison to the system formulated with $Cu^{II}Br_2$ initially (entry 2, solid and hollow squares).

Because of the effectiveness of dNbpy to provide a well-controlled polymerization, the versatility of this system was demonstrated with larger degrees of polymerization (DPs), monomers, and chain extension of a PMMA macroinitiator. Entries 6 and 7 summarize the results of two different targeted DPs. For all polymerizations, high conversions ($p \geq 80\%$), good correlations between $M_{n,theo}$ and $M_{n,GPC}$, narrow molecular weight distributions ($M_w/M_n \leq 1.3$), and high initiation efficiencies were obtained. When targeting a DP equal to 1000, slightly broader M_w/M_n and more discrepancy between predicted and experimental molecular weights were observed. A lower [$Cu^{II}Br_2$] limit may exist around 100 and 50 ppm of deactivator to maintain control in the dNbpy system. Figure 7a,b illustrates a constant concentration of radicals and constant number of polymer chains exist for each targeted degree of polymerization.

Investigation of Ethyl, Butyl, and *tert*-Butyl Methacrylate. Kinetic plots are shown in Figure 8a,b for EMA, BMA, and *t*BMA. In each case, monomer conversion increased with reaction time, whereas a constant concentration of propagating species was observed in the semilogarithmic plot ascertained from its linearity (Figure 8a). In addition, a constant number of polymer chains were observed for each monomer (Figure 8b), which was apparent from the linear relationship between number-average molecular weight and conversion. M_w/M_n values also decreased as the polymerization proceeded. Comparison of the apparent rate constants for each monomer revealed butyl methacrylate to be the largest. As expected, monomers with larger R groups have slightly higher k_p values in comparison to their smaller R group analogues.[53,54]

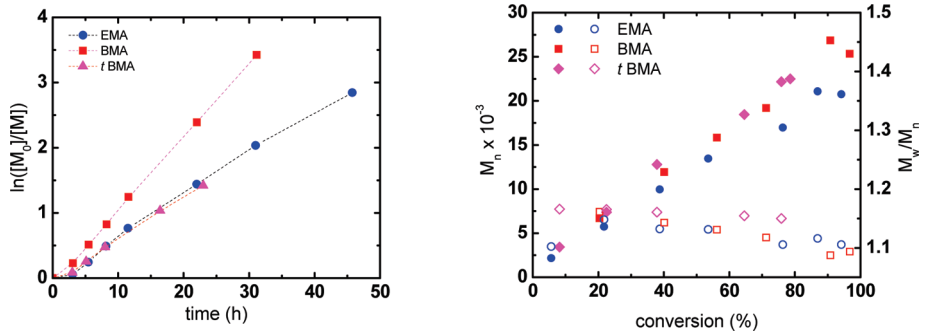

Figure 8. (a) First-order kinetic plot versus time; (b) evolution of molecular weight (solid) and molecular weight distribution (hollow) versus conversion as a function monomer. Polymerizations conducted in 50% (v/v) anisole at 35 °C. [M] = 4.55 M; monomer/EBPA/dNbpy/$Cu^{II}Br_2$ = 200/1/0.2/0.1; Cu^0: L = 10 mm, d = 1 mm (Table 2, entries 8−10).

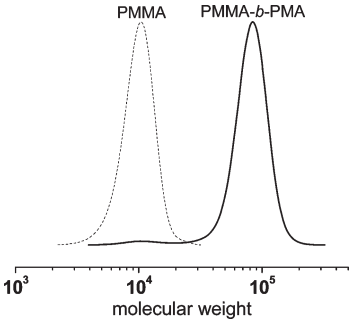

Figure 9. GPC chromatographs of the PMMA-Br macroinitiator (dashed line) and PMMA-*b*-PMA block copolymer (solid line). Macroinitiator synthesis and characterization (Table 2, entry 11) and block copolymer synthesis and characterization (Table 2, entry 12).

Chain Extension of PMMA-Br Macroinitiator. Livingness of the system was demonstrated by chain extending a PMMA macroinitiator with MA. PMMA macroinitiator was synthesized using the previously established polymerization conditions. Both reaction conditions and characterization of the resulting polymer are summarized in Table 2, entry 11. A subsequent PMA block was grown from the living chain end using PMDETA and $Cu^{II}Br_2$ in DMSO. DMSO was selected as the solvent for methyl acrylate because of its high K_{eq}.[55] A large degree of polymerization was targeted for the second block to provide substantial separation in GPC between the initial homopolymer and resulting block copolymer. The resulting block copolymer (PMMA-*b*-PMA) maintained a low M_w/M_n of 1.23 and $M_{n,GPC}$ close to the predicted value. Evidence of block copolymer formation can be seen in the GPC traces provided in Figure 9. A clear increase in molecular weight is visible, and absence of any appreciable amount of macroinitiator is apparent. This is further bolstered by a blocking efficiency value of ca. 94%.

Conclusions

ATRP of MMA and other methacrylates proceeded in a well-controlled fashion with both PMDETA and dNbpy in anisole at 35 °C. At high [$Cu^{II}Br_2$] and low [Cu^0]$_s$, the PMDETA-mediated system displayed characteristics of a living polymerization. Upon reduction of the deactivator concentration, an excess of ligand was required and polymerization rates were independent of the [$Cu^{II}Br_2$]. BPN was the most effective initiator, whereas EBPA and EBiB were either too active or inactive, respectively. ECPA initiator and $Cu^{II}Cl_2$ catalyst provided a significant improvement compared to EBPA/$Cu^{II}Br_2$ system. dNbpy proved to be an excellent ligand for ATRP of MMA when using copper wire over a range of catalyst concentrations and molecular weights. EMA, BMA, and *t*BMA monomers were all polymerized with an identical ATRP system, each resembling that of a controlled/living polymerization. Livingness was demonstrated by chain extension of PMMA-Br macroinitiator with MA and was found to be an effective method for the synthesis of block copolymers.

Acknowledgment. The authors thank the National Science Foundation (DMR 09-69301) and members of the CRP Consortium at Carnegie Mellon University for their financial support.

References and Notes

(1) Wang, J.-S.; Matyjaszewski, K. *J. Am. Chem. Soc.* **1995**, *117* (20), 5614–15.
(2) Wang, J.-S.; Matyjaszewski, K. *Macromolecules* **1995**, *28* (23), 7901–7910.
(3) Kato, M.; Kamigaito, M.; Sawamoto, M.; Higashimura, T. *Macromolecules* **1995**, *28* (5), 1721–3.
(4) Patten, T. E.; Xia, J.; Abernathy, T.; Matyjaszewski, K. *Science* **1996**, *272* (5263), 866–868.
(5) Kamigaito, M.; Ando, T.; Sawamoto, M. *Chem. Rev.* **2001**, *101* (12), 3689–3745.
(6) Tsarevsky Nicolay, V.; Matyjaszewski, K. *Chem. Rev.* **2007**, *107* (6), 2270–99.
(7) Matyjaszewski, K.; Tsarevsky, N. V. *Nature Chem.* **2009**, *1* (4), 276–288.
(8) Ouchi, M.; Terashima, T.; Sawamoto, M. *Chem. Rev.* **2009**, *109* (11), 4963–5050.
(9) Ando, T.; Kamigaito, M.; Sawamoto, M. *Macromolecules* **1997**, *30* (16), 4507–4510.
(10) Matyjaszewski, K.; Wei, M.; Xia, J.; McDermott, N. E. *Macromolecules* **1997**, *30* (26), 8161–8164.
(11) Wang, Y.; Matyjaszewski, K. *Macromolecules* **2010**, *43* (9), 4003–4005.
(12) Braunecker, W. A.; Itami, Y.; Matyjaszewski, K. *Macromolecules* **2005**, *38* (23), 9402–9404.
(13) Maria, S.; Stoffelbach, F.; Mata, J.; Daran, J.-C.; Richard, P.; Poli, R. *J. Am. Chem. Soc.* **2005**, *127* (16), 5946–5956.
(14) Brandts, J. A. M.; van de Geijn, P.; van Faassen, E. E.; Boersma, J.; Van Koten, G. *J. Organomet. Chem.* **1999**, *584* (2), 246–253.
(15) Min, K.; Matyjaszewski, K. *Cent. Eur. J. Chem.* **2009**, *7* (4), 657–674.
(16) Cunningham, M. F. *Prog. Polym. Sci.* **2008**, *33* (4), 365–398.
(17) Min, K.; Gao, H.; Yoon, J. A.; Wu, W.; Kowalewski, T.; Matyjaszewski, K. *Macromolecules* **2009**, *42* (5), 1597–1603.
(18) Min, K.; Gao, H.; Matyjaszewski, K. *J. Am. Chem. Soc.* **2005**, *127* (11), 3825–30.
(19) Min, K.; Yu, S.; Lee, H.-i.; Mueller, L.; Sheiko, S. S.; Matyjaszewski, K. *Macromolecules* **2007**, *40* (18), 6557–6563.
(20) Min, K.; Jakubowski, W.; Matyjaszewski, K. *Macromol. Rapid Commun.* **2006**, *27* (8), 594–598.
(21) Min, K.; Matyjaszewski, K. *Macromolecules* **2005**, *38* (20), 8131–8134.
(22) Min, K.; Matyjaszewski, K. *Macromolecules* **2007**, *40* (20), 7217–7222.

(23) Jakubowski, W.; Matyjaszewski, K. *Macromolecules* **2005**, *38* (10), 4139–4146.
(24) Jakubowski, W.; Matyjaszewski, K. *Angew. Chem., Int. Ed.* **2006**, *45* (27), 4482–4486.
(25) Jakubowski, W.; Min, K.; Matyjaszewski, K. *Macromolecules* **2005**, *39* (1), 39–45.
(26) Pietrasik, J.; Dong, H.; Matyjaszewski, K. *Macromolecules* **2006**, *39* (19), 6384–6390.
(27) Matyjaszewski, K. J., W.; Min, K.; Tang, W.; Huang, J.; Braunecker, W. A.; Tsarevsky, N. V. *Proc. Natl. Acad. Sci. U.S.A.* **2006**, *103*, 15309–15314.
(28) Lin, C. Y.; Coote, M. L.; Petit, A.; Richard, P.; Poli, R.; Matyjaszewski, K. *Macromolecules* **2007**, *40* (16), 5985–5994.
(29) Mueller, L.; Jakubowski, W.; Tang, W.; Matyjaszewski, K. *Macromolecules* **2007**, *40* (18), 6464–6472.
(30) Plichta, A.; Li, W.; Matyjaszewski, K. *Macromolecules* **2009**, *42* (7), 2330–2332.
(31) Mueller, L.; Matyjaszewski, K. *Macromol. React. Eng.* **2010**, *4* (3−4), 180–185.
(32) Zhang, L. F.; Miao, J.; Cheng, Z. P.; Zhu, X. L. *Macromol. Rapid Commun.* **2010**, *31* (3), 275–280.
(33) Matyjaszewski, K.; Coca, S.; Gaynor, S. G.; Wei, M.; Woodworth, B. E. *Macromolecules* **1997**, *30* (23), 7348–7350.
(34) Matyjaszewski, K.; Woodworth, B. E.; Zhang, X.; Gaynor, S. G.; Metzner, Z. *Macromolecules* **1998**, *31* (17), 5955–5957.
(35) Queffelec, J.; Gaynor, S. G.; Matyjaszewski, K. *Macromolecules* **2000**, *33* (23), 8629–8639.
(36) Matyjaszewski, K.; Pyun, J.; Gaynor, S. G. *Macromol. Rapid Commun.* **1998**, *19* (12), 665–670.
(37) Sarbu, T.; Matyjaszewski, K. *Macromol. Chem. Phys.* **2001**, *202* (17), 3379–3391.
(38) Matyjaszewski, K.; Dong, H.; Jakubowski, W.; Pietrasik, J.; Kusumo, A. *Langmuir* **2007**, *23* (8), 4528–4531.
(39) Percec, V.; Guliashvili, T.; Ladislaw, J. S.; Wistrand, A.; Stjerndahl, A.; Sienkowska, M. J.; Monteiro, M. J.; Sahoo, S. *J. Am. Chem. Soc.* **2006**, *128* (43), 14156–14165.
(40) Rosen, B. M.; Percec, V. *Chem. Rev.* **2009**, *109* (11), 5069–5119.
(41) Fleischmann, S.; Percec, V. *J. Polym. Sci., Part A: Polym. Chem.* **2010**, *48*, 2236–2242.
(42) Fleischmann, S.; Percec, V. *J. Polym. Sci., Part A: Polym. Chem.* **2010**, *48*, 2243–2250.
(43) Hornby, B. D.; West, A. G.; Tom, J. C.; Waterson, C.; Harrisson, S.; Perrier, S. *Macromol. Rapid Commun.* **2010**, *31* (14), 1276–1280.
(44) Destarac, M.; Boutevin, B. *Curr. Trends Polym. Sci.* **1999**, *4*, 201–223.
(45) Moad, G.; Solomon, D. H. *The Chemistry of Radical Polymerization*, 2nd revised ed.; Elsevier: Oxford, 2006; p 635.
(46) Destarac, M.; Matyjaszewski, K.; Boutevin, B. *Macromol. Chem. Phys.* **2000**, *201* (2), 265–272.
(47) Matyjaszewski, K.; Tsarevsky, N. V.; Braunecker, W. A.; Dong, H.; Huang, J.; Jakubowski, W.; Kwak, Y.; Nicolay, R.; Tang, W.; Yoon, J. A. *Macromolecules* **2007**, *40* (22), 7795–7806.
(48) Tsarevsky, N. V.; Braunecker, W. A.; Matyjaszewski, K. *J. Organomet. Chem.* **2007**, *692* (15), 3212–3222.
(49) Tsarevsky, N. V.; Braunecker, W. A.; Tang, W.; Matyjaszewski, K. *ACS Symp. Ser.* **2009**, *1023*, 85–96.
(50) Kwak, Y.; Matyjaszewski, K. *Polym. Int.* **2009**, *58* (3), 242–247.
(51) Tang, W.; Kwak, Y.; Braunecker, W.; Tsarevsky, N. V.; Coote, M. L.; Matyjaszewski, K. *J. Am. Chem. Soc.* **2008**, *130* (32), 10702–10713.
(52) Nanda, A. K.; Matyjaszewski, K. *Macromolecules* **2003**, *36* (22), 8222–8224.
(53) Beuermann, S.; Buback, M. *Prog. Polym. Sci.* **2002**, *27* (2), 191–254.
(54) Barner-Kowollik, C.; Russell, G. T. *Prog. Polym. Sci.* **2009**, *34* (11), 1211–1259.
(55) Braunecker, W. A.; Tsarevsky, N. V.; Gennaro, A.; Matyjaszewski, K. *Macromolecules* **2009**, *42* (17), 6348–6360.